ORGANOMETALLICS

pubs.acs.org/Organometallics

Article

Group 11 Bis(alumanyl)metallates

Han-Ying Liu, Jakub Kenar, Samuel E. Neale, Marta Garofalo, Michael S. Hill,* Claire L. McMullin,* Mary F. Mahon,* and Emma Richards

Cite This: https://doi.org/10.1021/acs.organomet.4c00460

Read Online

ACCESS | Metrics & More | Article Recommendations | Supporting Information

ABSTRACT: Reactions of the coinage metal (CM) cyanides, CuCN, AgCN, or K[Au(CN)$_2$], with [{SiN^{Dipp}}AlK]$_2$ ({SiN^{Dipp}} = {CH$_2$SiMe$_2$N(Dipp)}; Dipp = 2,6-*i*-Pr$_2$C$_6$H$_3$) result in KCN metathesis and a series of "alumina-Gilman" reagents, [({SiN^{Dipp}}Al)$_2$CM]K (CM = Cu, Ag, or Au). The latter species may be isolated in both charge-separated, [({SiN^{Dipp}}Al)$_2$CM]$^-$[K(THF)$_6$]$^+$, or contact ion pair forms when crystallized in the presence or absence of THF. Computational analysis apportions a high degree of covalency to the CM−Al metal bonding and attribution of an aluminum oxidation state that is best represented as Al(II). This latter inference is supported by the experimental observation of THF activation, deduced to result from the competitive single electron reduction of the group 11 center during the synthesis of the bis(alumanyl)metalates. UV photolysis of [({SiN^{Dipp}}Al)$_2$Ag]K provided a product of 2-fold Al(II) radical addition to benzene. This species is also synthesized by a modification of the reaction that gave rise to the initially identified cuprate metathesis product. The intermediacy of [{SiN^{Dipp}}Al$^{\bullet}$] radicals, which are proposed to add to benzene in a stepwise manner, is supported by the observation of *in situ* recorded EPR spectra, the simulated parameters of which have been assigned to the singly aluminated benzene product, [{SiN^{Dipp}}Al(C$_6$H$_6$)$^{\bullet}$].

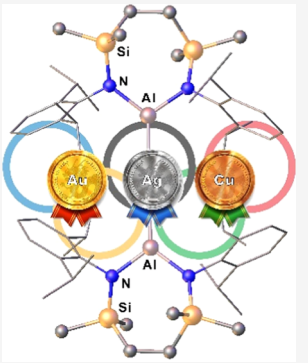

INTRODUCTION

Organocuprates, either as the homoleptic Gilman reagents, [R$_2$Cu]$^-$M$^+$ (where R = e.g., alkyl, alkenyl, aryl and M = alkali metal, typically Li), or in heterocuprate, [RCu(X)]$^-$M$^+$ (X = nontransferable anion, e.g., halide, heteroatom anion, cyanide) form, serve as a uniquely effective means for the delivery of hard carbanions to softer electrophilic substrates.[1−3] The potential utility of charge neutral Cu−E-bonded species derived from carbon's heavier tetravalent group 14 congeners (E = Si,[4−14] Ge,[15−20] Sn[21,22]) has also been recognized,[23] and a handful of directly related tetrelidocuprates, i.e., [(R$_3$E)$_2$Cu]$^-$M$^+$ or [(R$_3$E)CuX]$^-$M$^+$ (E = Si,[24−29] Ge[30,31]), have been characterized. Irrespective of the identity of the group 14 anion, however, a majority of this chemistry is achieved by reaction of the appropriate alkali metal tetrelide with either a copper(I) halide or cyanide.

Broadly analogous molecules comprising group 13-to-copper σ bonds have also, more recently, become accessible through the development of a suite of nucleophilic boron- (e.g., **I**, Figure 1),[32−34] aluminum- (e.g., **II**−**IV**),[35−42] gallium- (e.g., **V**, **VI**, **VII**)[35,43−45] and indium-centered (e.g., **VIII**, **IX**) anions.[46,47] While reactions of such reagents with phosphine- or carbene-coordinated Cu(I) halides have enabled the synthesis of several two-coordinate neutral species (e.g., **X** and **XI**),[34,48−55] trielide-based cuprates are only represented by three lithium borylcopper bromide or cyanide derivatives of **I**[48−50] and the potassium bis-alumanyl complex (**XII**), which provides a unique example of a "Gilman-type" group 13 homocuprate.[56] The resistance to reduction and the apparent subversion of nobility in the presence of two electron-releasing aluminum centers of the copper center in **XII** (Cu$_{(aq)}^+$ + e$^-$ → Cu$_{(s)}$; E^0 = +0.52 V) is remarkable and raises questions with regard to the importance of the polyhapto arene-potassium interactions intrinsic to its contact ion pair structure and the potentially stabilizing influence of the consequent close contact between the copper and K$^+$ centers [Cu···K 3.0669(6) Å].[56]

A limited number of charge neutral gold and silver derivatives analogous to **X** and **XI** have also been prepared,[55−57] and it is notable that the polarization of the group 11-aluminum interactions (i.e., {Cu/Ag/Au}$^{\delta-}$-Al$^{\delta+}$) can confer similar nucleophilic character to each of the coinage metals (CM). While a variety of solid-state auride (i.e., formal Au$^-$) species have long been known,[58] consideration of the relevant reduction potentials (Ag$_{(aq)}^+$/Ag, E^0 = +0.80 V; Au$_{(aq)}^+$/Au, E^0 = +1.83 V) and the consequent accumulation of negative charge, therefore, implies the realization of heavier group 11 analogues of compound **XII** presents an increasingly unlikely proposition. In this contribution, however, we confirm the accessibility of the complete range of "Gilman-type" potassium group 11 bis(alumanyl)metalate derivatives, both with and without the contacting presence of the group 1 cation. We also demonstrate that metathetical CM−Al bond formation is kinetically competitive with the (anticipated)

Received: October 29, 2024
Revised: November 11, 2024
Accepted: November 20, 2024

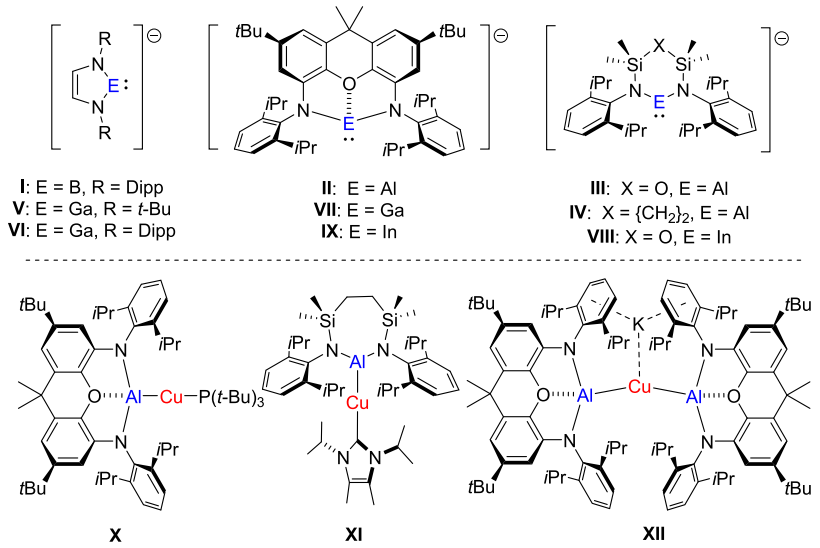

Figure 1. Selected group 13-centered anions (**I**–**IX**; Dipp = 2,6-*i*-$Pr_2C_6H_3$) and copper alumanyl species (**X**–**XII**).

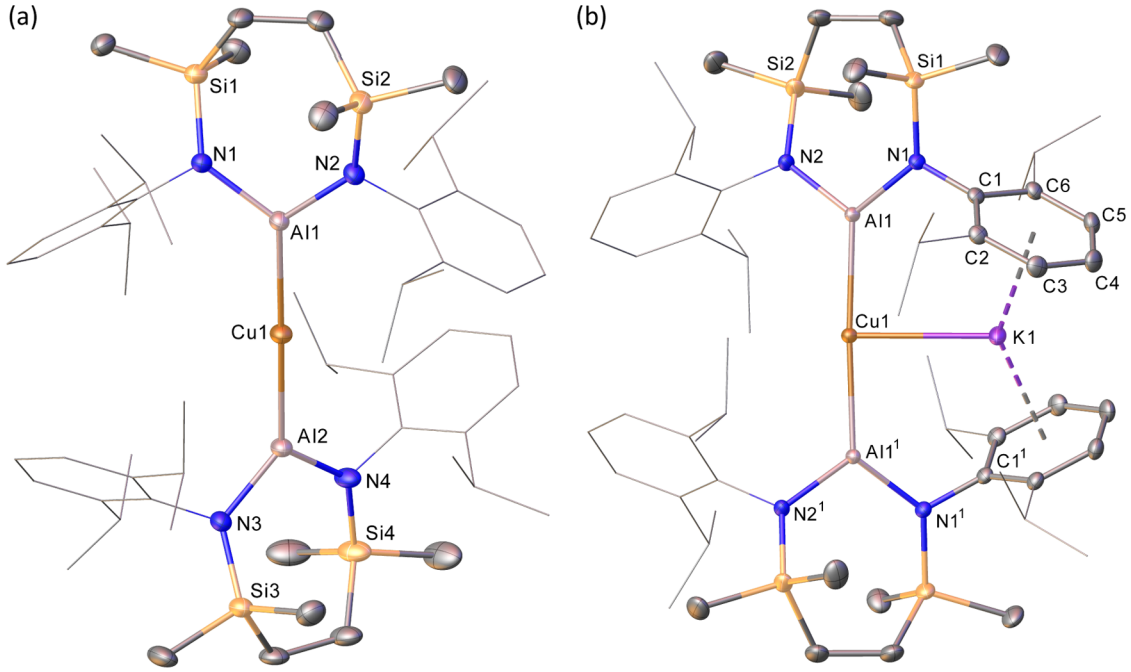

Figure 2. (a) Plot depicting the structure of one of the two copper-based entities present in the asymmetric unit of **2**. Ellipsoids are shown at 30% probability. Cations, hydrogen atoms and minor disordered components have been omitted, for clarity. Peripheral substituents are depicted as wireframes, also for visual ease. (b) Plot depicting the structure of **4**. Ellipsoids are shown at 30% probability. Solvent, minor disordered components and hydrogen atoms have been omitted for perspicuity. Peripheral substituents are depicted as wireframes, also for visual ease. Symmetry operation: [1] $1 - x, y, {}^{3}/_{2} - z$.

products of noble metal reduction. Furthermore, this process may be photochemically and chemically initiated, in both instances to enable the governable generation of reactive Al(II) species.

RESULTS AND DISCUSSION

Synthesis of Potassium Group 11 Bis(alumanyl)-metallates. Our entry point to this chemistry arose from a serendipitous observation provided by the attempted synthesis of a potassium aluminocyanocuprate derived from the alumanyl anion **IV** (Figure 1). Sonication of a reaction of $[\{SiN^{Dipp}\}AlK]_2$ (**1**: $\{SiN^{Dipp}\}$ = $\{CH_2SiMe_2N(Dipp)\}_2$; Dipp = 2,6-*i*-$Pr_2C_6H_3$) and CuCN in THF for 24 h resulted in the decolorization of the initial bright yellow solution. Interrogation of the resultant solution by ^{1}H NMR spectroscopy confirmed the complete consumption of the alumanyl starting material and the formation of a predominant product (**2**), which was estimated to comprise *ca.* 70% of the total $\{SiN^{Dipp}\}$-containing species in solution. Compound **2** displayed evident C_2 symmetry giving rise to a single Dipp *iso*-propyl methine environment at δ 3.72 ppm. Although the presence of a second component (**3**) could be inferred from this initial analysis, an interpretation of its structure by NMR spectroscopy was prevented by its asymmetry that was apparent from the analogous $\{SiN^{Dipp}\}$ ligand methine region

https://doi.org/10.1021/acs.organomet.4c00460
Organometallics XXXX, XXX, XXX–XXX

Scheme 1. Reaction of 1 with CuCN in THF Yielding Compounds 2 and 3

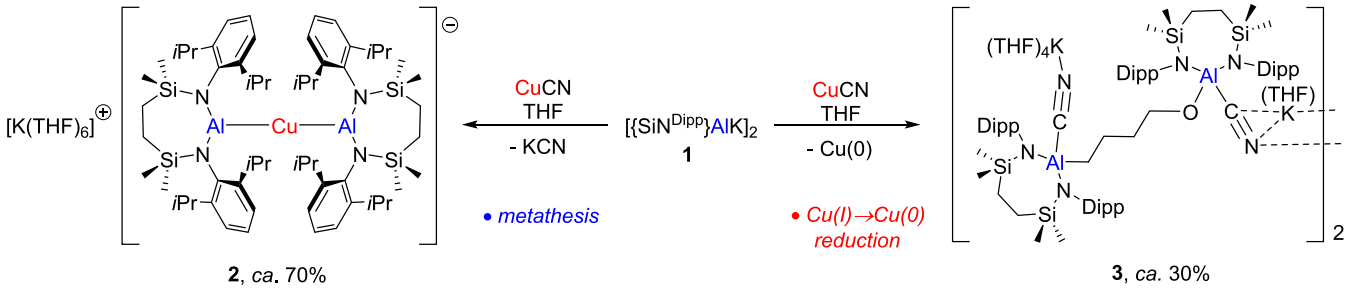

Table 1. Selected Bond Lengths (Å) and Angles (deg) of Group 11 Bis(alumanyl)metallates, 2, 4−6, and 9

	2[a]	4[a]	5[b]	6[b]	9[c]
Al1−M1	2.4141(10)[d]	2.4588(3)	2.5641(7)	2.5776(8)	2.5065(9)
Al2−M1	2.4139(10)[e]		2.5626(8)		
M1−K1		3.0057(4)		3.1594(9)	3.0991(9)
Al1−N1	1.865(3)[f]	1.8700(10)	1.867(2)	1.864(2)	1.858(2)
Al1−N2	1.869(3)[g]	1.8497(10)	1.870(2)	1.850(2)	1.844(3)
Al2−N3	1.876(3)[h]		1.865(3)		
Al2−N4	1.860(3)[i]		1.878(3)		
Al1−M1−Al2	179.04(4)[j]	176.793(18)[m]	178.12(3)	177.21(3)[n]	178.48(4)[p]
N1−Al1−N2	108.15(13)[k]	110.14(5)	107.70(10)	110.86(10)	110.19(12)
N3−Al2−N4	108.78(14)[l]		107.81(11)		

[a]M = Cu. [b]M = Ag. [c]M = Au. [d]Al3−Cu2 2.4107(10) Å. [e]Al4−Cu2 2.4137(10) Å. [f]Al3−N5 1.871(3) Å. [g]Al3−N6 1.867(3) Å. [h]Al4−N7 1.869(3) Å. [i]Al4−N8 1.869(3) Å. [j]Al3−Cu2−Al4 176.99(4)°. [k]N5−Al3−N6 108.64(13)°. [l]N7−Al4−N8 108.47(13)°. [m]Al1−Cu1−Al1[1]. [n]Al1−Ag1−Al1[1]. [p]Al1−Au1−Al1[1].

Scheme 2. Inter-convertibility of Compounds 2 and 4 and the Rational Synthesis of 4

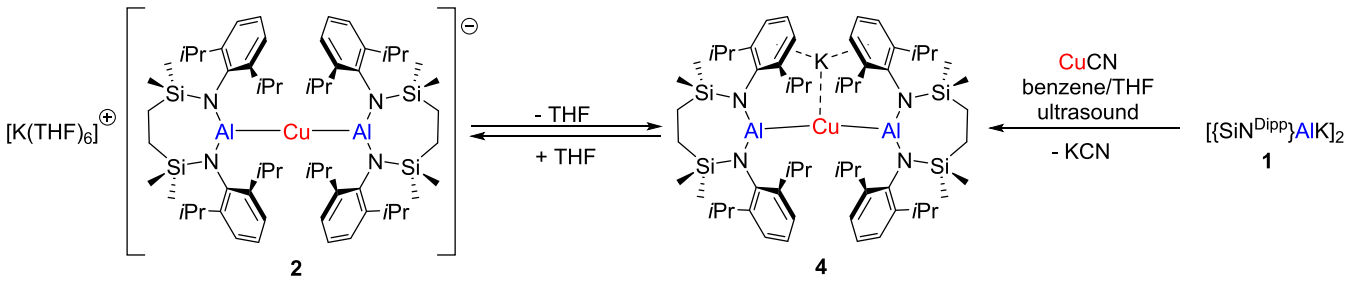

and which appeared as a more complex series of multiplets resonating between δ 4.25 and 3.67 ppm.

The subsequent identification of both compounds **2** and **3** was achieved by the application of conditions appropriate for their selective crystallization. While the formation of colorless single crystals of **2** was accomplished in 52% isolated yield by diffusion of hexane into the reaction solution, the isolation of **3** required the slow evaporation of the resultant supernatant solution at room temperature. In both cases, the origin of the solution-state observations was made evident by single crystal X-ray diffraction analysis. Although compound **2** is a potassium bis(alumanyl)cuprate, unlike the contact ion-paired formulation of the earlier described derivative, **XII**,[56] its preparation in the coordinating solvent THF results in the generation of a charge-separated ionic formulation, $[(\{SiN^{Dipp}\}Al)_2Cu]^-[K(THF)_6]^+$, comprising two otherwise unsupported Cu−Al σ bonds (Figure 2, Scheme 1). In contrast, the side product (**3**) does not contain the group 11 element, but is a centrosymmetric potassium cyanoaluminate dimer, $[(\{SiN^{Dipp}\}Al\{C{\equiv}NK(THF)_4\})\{(CH_2)_4O\}(\{(THF)KN{\equiv}C\}Al\{SiN^{Dipp}\})]_2$, of two dialuminum products of THF solvent activation (Figure 2, Scheme 1). Selected bond length and angle data for **2** are presented in Table 1, while those for **3** are provided in the relevant figure caption.

Although a redissolved sample of compound **2** in d_8-THF provided NMR spectra consistent with the C_2-symmetric species identified in the initial *in situ* reaction mixture, exposure of the isolated crystals to vacuum for two hours induced their decrepitation. Analysis of the resultant colorless powder by NMR spectroscopy in C_6D_6 evidenced the complete disappearance of any signals arising from THF and the generation of a single new compound (**4**, Scheme 2). Unlike compound **XII**, which displayed evidence of a lower symmetry and the maintenance of its solid-state structure on the NMR time scale, the ^{1}H NMR spectrum of **4** continued to present a single, albeit unresolved, resonance arising from the $\{SiN^{Dipp}\}$ *iso*-propyl methine protons (δ 3.90 ppm). Despite this contrast, indicative of a greater lability of structure, slow evaporation of the benzene solvent provided single crystals for analysis by X-ray crystallography, the results of which revealed that **4** was a further contact ion-paired variant of **2** but with a structure more analogous to that of **XII** (Figure 2, Table 1).

While the asymmetric unit of **4** comprises a single centrosymmetric heterobimetallic molecular structure in

https://doi.org/10.1021/acs.organomet.4c00460
Organometallics XXXX, XXX, XXX−XXX

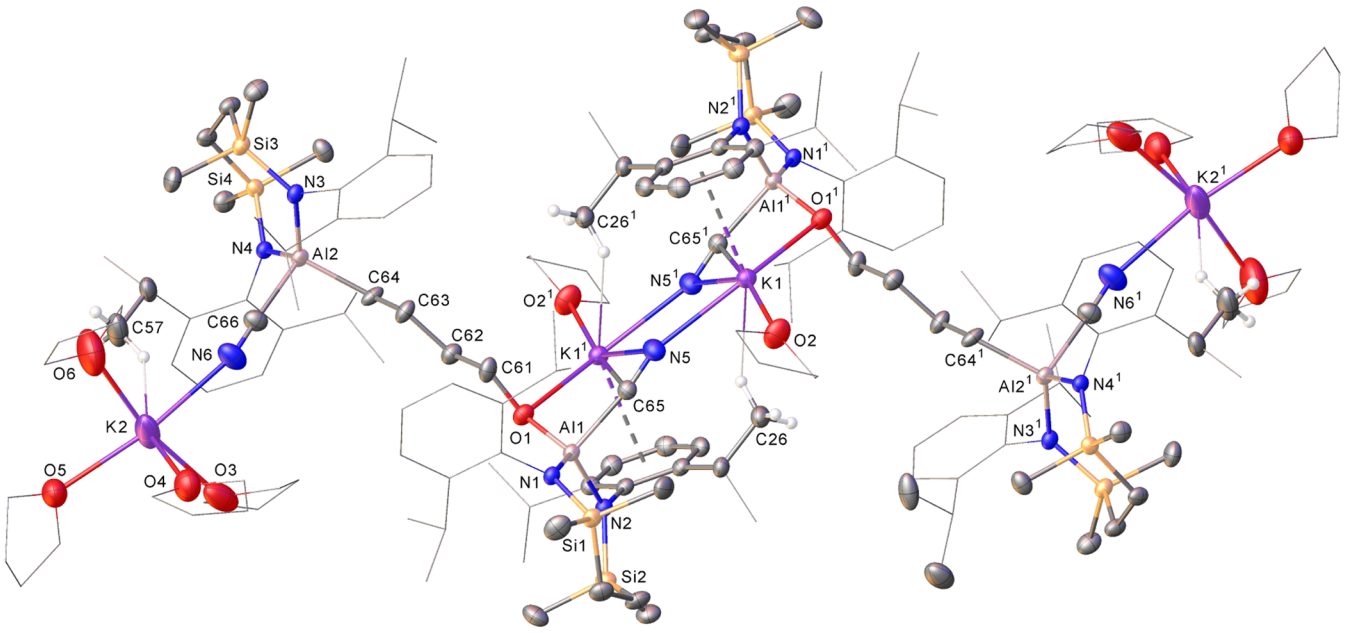

Figure 3. Plot depicting the structure of **3**. Ellipsoids are shown at 30% probability. Minor disordered components and hydrogen atoms (those attached to C26 and C57, excepted) have been omitted for clarity. Peripheral substituents are depicted as wireframes, also for visual ease. Symmetry operation: $^1 1 - x, 1 - y, - z$. Selected bond lengths (Å) and angles (deg) for **3**: Al1−O1 1.7275(18), Al1−N1 1.8350(19), Al1−N2 1.857(2), Al1−C65 2.006(3), Al2−N3 1.870(2), Al2−N4 1.871(2), Al2−C66 2.022(3), Al2−C64 1.958(4), N5−C65 1.157(4), N6−C66 1.150(4), N1−Al1−N2 114.82(9), N3−Al2−N4 113.70(9).

which K1 is encapsulated by polyhapto interactions with a single Dipp substituent of each [{SiN^{Dipp}}Al] moiety, that of **2** contains two unique ion pairs. The most relevant bond lengths and angles across both anionic components of **2** are, however, very similar (Table 1). The following discussion, thus, refers solely to the Cu1-containing anion (Figure 2). Despite the contrasting disposition of the alkali metal cations in the structures of **2** and **4**, the introduction of potassium within the coordination sphere of **4** results in only a marginal elongation of the Cu−Al bonds [**2**, Cu1−Al1 2.4141(10), Cu1−Al2 2.4139(10) Å; **4**, Cu1−Al1 2.4588(3) Å]. These values and the angles subtended by the three contiguous metal centers [**2**, Al1−Cu1−Al2 179.04(4)°; **4**, Al1−Cu1−Al1^1 176.793(18) Å] are also closely comparable to the corresponding metrics presented by compound **XII** [Cu−Al 2.4076(5), 2.4075(5) Å; 174.88(2)°].[56] While the slight contraction of the latter bonds possibly reflects the higher energy Al-centered HOMO of the alumanyl anion **II** in comparison to that donated by the 7-membered chelate structure of **IV**,[39] the totality of these data are indicative of very similar electronic structures across all three cuprate species. Despite the high mutual trans influence exerted by each alumanyl moiety in both compounds **2** and **4**, their Cu−Al bond lengths are also only marginally elongated in comparison to those of similarly low-coordinate species such as **XI** [2.3449(4) Å], the cyclic alkylamino carbene derivative [{SiN^{Dipp}}AlCu(^{Me2}CAAC)] (^{Me2}CAAC = 1-(2,6-di-*iso*propyl-phenyl)-3,3,5,5-tetra-methylpyrrolidin-2-ylidene) [2.4028(7) Å][51] and the phosphine-adducted [{SiN^{Dipp}}AlCu(P*t*-Bu$_3$)] [2.3755(3) Å].[55]

Further investigation of the solution behavior of **4** revealed that its dissolution in THF resulted in the immediate reformation of compound **2** (Scheme 2). Similarly, the direct and exclusive synthesis of compound **4** could be achieved through performance of the reaction of **1** with CuCN in benzene, but with the addition of a limited quantity of THF and under ultrasonic conditions to enhance the solubility of the Cu(I) reagent. Although we have not further investigated the nature of this interconvertibility, we have previously attempted, without success, to access such metalate species in a similar manner to that reported for **XII** via copper(I) halide starting materials. While it is apparent that both forms of bis(alumanyl)cuprate are energetically similar, the CuCN performs an analogous role in both syntheses, possessing the appropriate solubility to modulate the kinetics of 2-fold Cu−Al bond formation with only limited side reaction, while providing a suitable thermodynamic driving force for metathesis through the production of the presumed KCN side product. Isolated samples of both compounds **2** and **4** displayed notable thermal stability, with solutions showing no indication of decomposition even when heated to 80 °C for extended periods of time.

The molecular structure of compound **3** (Figure 3) is a centrosymmetric dimer of bimetallic species, each of which comprise two [{SiN^{Dipp}}Al] moieties connected by a [(CH$_2$)$_4$O]$^{2-}$ dianion arising from the ring opening of a molecule of THF solvent. The Al1-containing unit is connected to the (O1) oxygen of this latter ligand while Al2 interacts with the terminal methylene (C64). Both unique *pseudo*-tetrahedral aluminum centers are further coordinated by an equivalent of *C*-bound KCN, which differ through the number of molecules of THF coordinated to each potassium atom. K2 interacts with four molecules of *O*-donor solvent and is further coordinated by the (N6) nitrogen center of the Al2-bound cyanide with a close contact to a methyl group of a {SiN^{Dipp}} *iso*-propyl substituent. In contrast, K1 is coordinated by a single molecule of THF, an η^2-*C*,*N*-interaction [C65−K1^1 3.092(2); N5−K1^1 3.265(3) Å] to the Al1-coordinated nitrile and by O1 of the alkoxyalkyl ligand [K1−O1^1 2.894(2) Å]. Dimer propagation is then achieved through two crystallographically equivalent K-μ_2−N-K [K1−N5 2.785(3) Å]

https://doi.org/10.1021/acs.organomet.4c00460
Organometallics XXXX, XXX, XXX−XXX

Scheme 3. Synthesis of Compounds 3, 5, 6, and 7 from the Reaction of 1 and AgCN

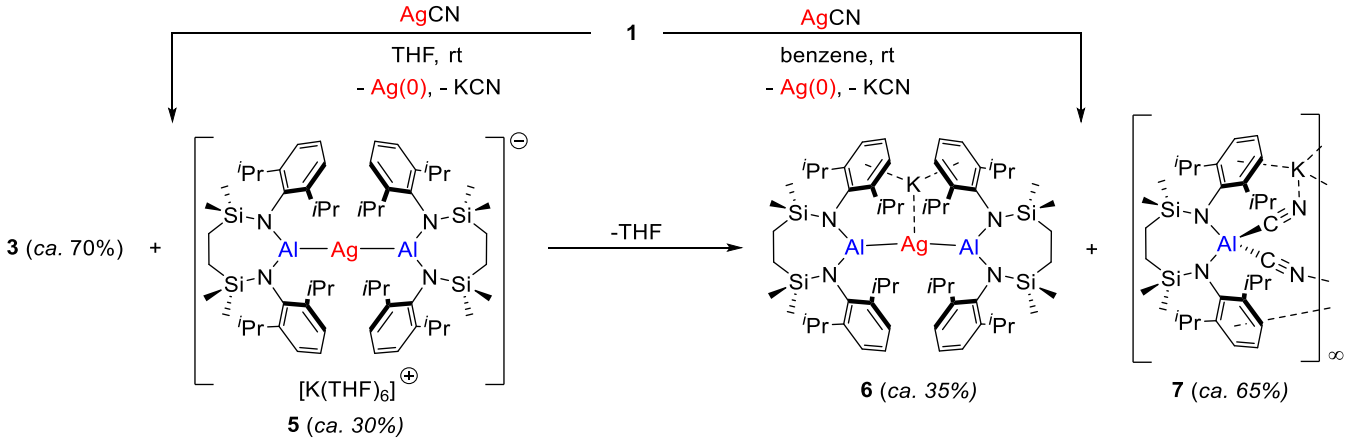

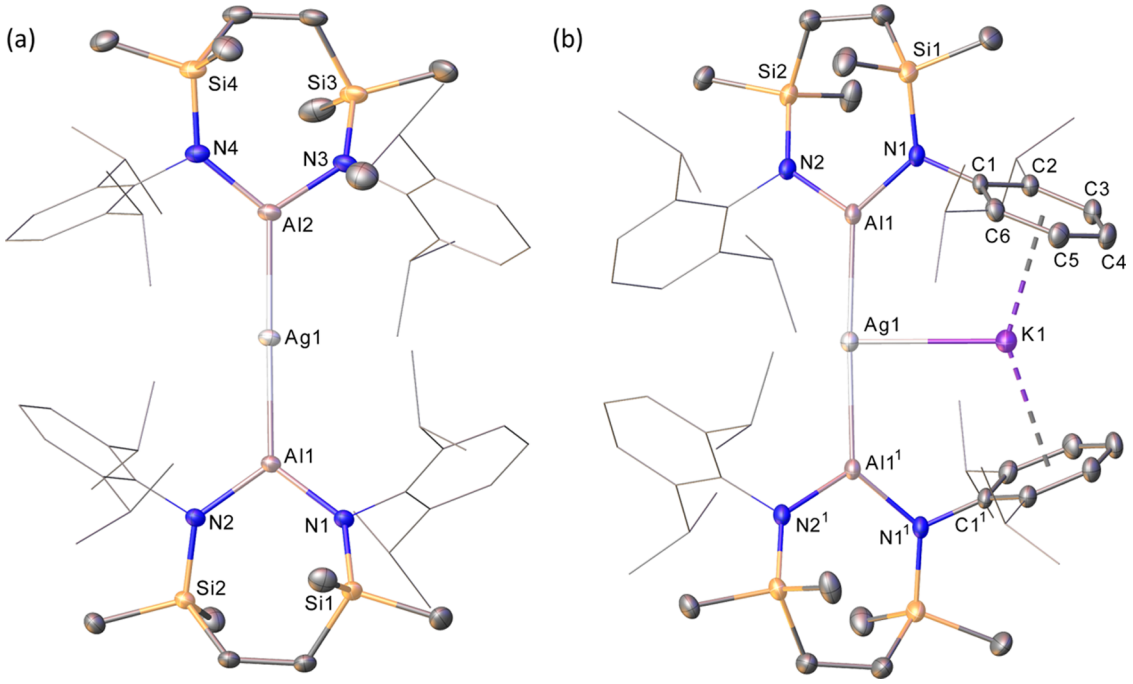

Figure 4. (a) Plot depicting the structure of the anion present in the asymmetric unit of **5**. Ellipsoids are shown at 30% probability. The cation, solvent and hydrogen atoms have been omitted, for clarity, while peripheral substituents are depicted as wireframes, for similar reasons. (b) Plot depicting the structure of **6**. Ellipsoids are shown at 30% probability. Solvent and hydrogen atoms have been omitted, and peripheral substituents are depicted as wireframes, for clarity. Symmetry operation: ^{1} x, $1/2 - y$, $^{3}/_{2} - z$.

bridging interactions, such that each aggregate comprises four [{SiN^{Dipp}}Al] moieties. The incorporation of KCN in the structure of **3** validates its role as the assumed metathetical byproduct formed during the synthesis of compounds **2** and **4** (Schemes 1 and 2). Furthermore, we hypothesize that the generation of the THF-derived alkoxyalkyl chain in **3** is most likely a radical-based process and implies that Cu(I) reduction and single electron oxidation of the Al(I) center of **1** provides a pathway for Al(II) generation that is competitive with the group 11 cyanide metathesis (Scheme 1 and *vide infra*).

This latter hypothesis is also consistent with our subsequent extension of this cyanide-based protocol to the heavier members of the group 11 triad. Storage of a reaction performed at room temperature between compound **1** and AgCN in THF for 24 h resulted in the decolorization of the initial bright yellow solution and the deposition of a significant quantity of gray precipitate, assumed to be silver metal. Analysis of the now colorless solution by NMR spectroscopy again revealed the production of two predominant species in an approximate 7:3 ratio (Figure S6), the major of which presented an identical ^{1}H NMR spectrum as the THF activation side product (**3**) observed during the synthesis of compound **2** (Scheme 3). The minor component of the solution (**5**) also displayed a spectroscopic signature that was strongly reminiscent of that provided by **2**, albeit with some minor perturbations to the observed chemical shifts for each {SiN^{Dipp}} ligand environment. The separation of the two major components of the reaction was achieved in a similar manner to that applied to the analogous copper-based reaction, whereupon diffusion of hexane and slow evaporation of the subsequent supernatant, respectively, were found to provide viable quantities of colorless single crystals of the charge-separated bis(alumanyl)argentate (**5**, 23% isolated yield) and the product of THF activation (**3**).

https://doi.org/10.1021/acs.organomet.4c00460
Organometallics XXXX, XXX, XXX−XXX

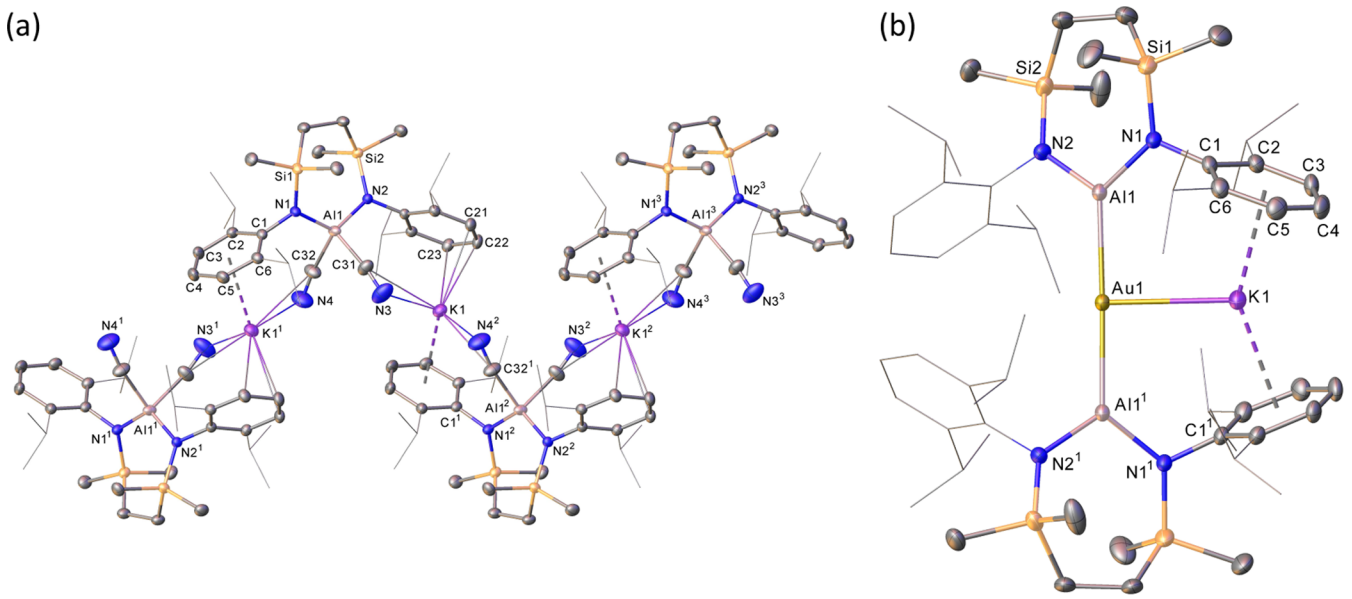

Figure 5. (a) Plot depicting the structure of **7**. Ellipsoids are shown at 30% probability. Solvent, minor disordered components and hydrogen atoms have been omitted for perspicuity. Peripheral substituents are depicted as wireframes, also for visual ease. Symmetry operations: [1] $2 - x, -1/2 + y, 1/2 - z$; [2] $2 - x, 1/2 + y, 1/2 - z$; [3] $x, 1 + y, z$. Selected bond lengths (Å) and angles (deg): Al1−N1 1.8275(19), Al1−N2 1.8265(19), Al1−C32 1.982(3), Al1−C31 1.953(3), K1−N3 2.647(4), K1−N4[1] 2.723(4), N2−Al1−N1 119.66(9), C31−Al1−C32 91.25(16). (b) Plot depicting the structure of **9**. Ellipsoids are shown at 30% probability. Solvent, minor disordered components and hydrogen atoms have been omitted for visual ease. Similarly, peripheral substituents are depicted as wireframes, for clarity. Symmetry operation: [1] $x, {}^{3}/_{2} - y, 1/2 + z$.

Scheme 4. Reactivity of 1 toward K[Au(CN)$_2$] and the Synthesis of Compounds 8 and 9

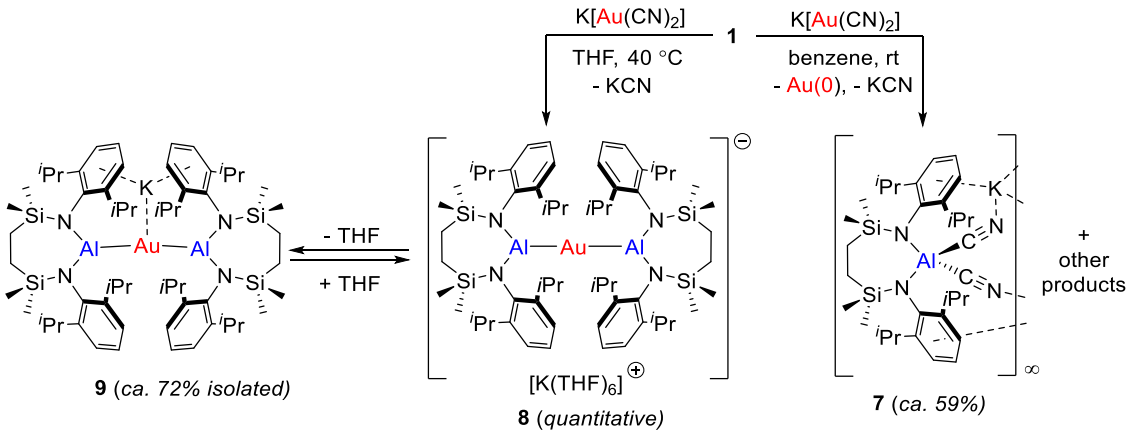

While the isolation of the byproduct (**3**) was confirmed by a unit cell check, X-ray diffraction analysis established that **5**, though not isostructural in comprising a single unique cation/anion pair in its asymmetric unit, is otherwise analogous to compound **2** (Figure 4). Although the preparation of the silver analogue of compound **X** (Figure 1) has been described,[56] the sole structurally characterized precedent comprising an unsupported Ag−Al bond is provided by [(^{Cy}CAAC)AgAl{SiNDipp}] (^{Cy}CAAC = 2-[2,6-bis(1-methylethyl)phenyl]-3,3-dimethyl-2-azaspiro[4.5]dec-1-ylidene).[55] As observed for the structures of **2** and **4**, the mutual trans influence imposed across the almost linear Al−Ag−Al array [Al1−Ag1−Al2 178.12(3)°] results in a significant elongation of the Al−Ag bonds of the anionic component of **5** [Al1−Ag1 2.5641(7); Al2−Ag1 2.5626(8) Å] in comparison to that of the neutral carbene adduct [2.4694(6) Å].

In contrast to the stability presented by **2** and **4**, isolated samples of compound **5** were found to be highly prone to deposition of metallic silver and other intractable products even at room temperature in the dark. A pure sample could, however, be stored at −30 °C for more than 1 week without any apparent decomposition. Furthermore, slow evaporation of the THF reaction solvent provided several orange crystals, which were identified as the potassium argentate contact ion pair analogue of **4**, compound **6** (Scheme 3). Although it is evident from this observation that, like the transformation of **2** to **4**, compound **5** is prone to the loss of THF from potassium, compound **6** could also be prepared from a d_6-benzene solution of **1** and AgCN, with or without addition of limited amounts of THF, after sonication for 6 h and in the absence of light. This procedure yielded an orange solution, which, by ^{1}H NMR spectroscopy, was judged to comprise *ca.* 35% of the contact ion pair derivative along with (*ca.* 65%) of a further side product (**7**, Scheme 3). Both compounds were identified by X-ray diffraction analysis, which confirmed the constitution of **6** (Figure 4, Table 1) and identified compound **7** as the

https://doi.org/10.1021/acs.organomet.4c00460
Organometallics XXXX, XXX, XXX−XXX

Table 2. Selected BCP and Atomic Data for 2′, 4, 5′, 6, 8′, and 9 Computed at the BP86/BS2//BP86/BS1 Level of Theory[a]

complex	BCP (A−B)	R_{A-B}	$\rho(r)$	$\nabla^2\rho(r)$	$H(r)$	q_A	q_B
4	Cu−K	3.08	0.0129	0.0366	0.0005	−0.50	+0.81
	Cu−Al	2.51	0.0526	−0.0400	−0.0202		+1.50
	Cu−H	2.36	0.0164	0.0363	−0.0005		+0.01
2′	Cu−Al	2.49	0.0532	−0.0378	−0.0205	−0.40	+1.46
	Cu−H	2.57	0.0114	0.0241	0.0001		+0.03
6	Ag−K	3.20	0.0128	0.0389	0.0007	−0.63	+0.82
	Ag−Al	2.62	0.0514	−0.0334	−0.0191		+1.56
	Ag−H	2.71	0.0108	0.0250	0.0004		+0.01
5′	Ag−Al	2.59	0.0534	−0.0358	−0.0208	−0.57	+1.54
	Ag−H	2.70	0.0112	0.0259	0.0004		+0.03
9	Au−K	3.16	0.0156	0.0525	0.0011	−1.28	+0.83
	Au−Al	2.57	0.0575	−0.0226	−0.0264		+1.87
	Au−H	2.74	0.0119	0.0293	0.0006		+0.03
8′	Au−Al	2.54	0.0598	−0.0160	−0.0278	−1.23	+1.85
	Au−H	2.68	0.0084	0.0194	0.0005		+0.05

[a]Distances are in Å, electron density units are in e bohr^{-3}, and energy units are in Hartrees.

potassium dicyanoaluminate, [{SiN^{Dipp}}Al(CN)$_2$K] (Figure 5, with selected bond lengths and angles provided in the figure caption). Although, again, we have no compelling rationale for the predominant formation of this latter product under these conditions, its identification also provides a strong mitigation for the necessary Ag(I) reduction and KCN metathesis processes evoked in Scheme 3. As observed for the cuprate analogues, **2** and **4**, the introduction of the potassium cation to the proximity of the silver center [Ag1−K1 3.1594(9) Å] in **6** appears to exert very little influence over the group 11-aluminum interactions. The Al-M bonds are only marginally elongated [2.5776(8) Å] while the Al1−Ag1−Al^1 angle [177.21(3)°] is only slightly distorted from linearity.

The commercial unavailability of AuCN dictated that an extension of this chemistry to the heaviest member of group 11 required the use of potassium dicyanoaurate(I) as an appropriate gold starting material. Accordingly, addition of d_8-THF to a mixture of **1** and K[Au(CN)$_2$] and heating to 40 °C provided a dark red solution, which was interpreted to indicate the likely formation of gold nanoparticles. Irrespective of this observation, analysis of the resultant solution by ^{1}H and ^{13}C NMR spectroscopy and comparison to the corresponding data provided by compounds **2** and **5** was indicative of the almost exclusive formation of the charge-separated ion pair potassium bis(alumanyl)aurate, [({SiN^{Dipp}}Al)$_2$Au]$^-$[K(THF)$_6$]$^+$ (**8**, Scheme 4). Although the identity of this compound may be assigned with a high level of confidence, all attempts to obtain suitable single crystals for X-ray analysis were unsuccessful. Rather, either slow evaporation of the reaction solution or simple removal of volatiles again induced the complete exclusion of coordinating THF and the isolation of its contact ion pair equivalent (**9**), the solid-state structure of which was again identified by single crystal X-ray diffraction analysis (Figure 5, Table 1). As established for both copper and silver, the adoption of the *transoid* bis(alumanyl)metalate structure results in a minor elongation of the relevant Au−Al bonds [Au1−Al1 2.5065(9) Å] in comparison to those observed in either of the direct gold-centered analogues of the copper compounds **X** [2.402(3) Å][57] or **XI** [2.369(2) Å] that have been described.[55] Similarly, the Al1−Au1−Al1^1 bond angle [178.48(4)°] approaches linearity despite the close proximity of gold to potassium [Au1−K1 3.0991(9) Å], a distance which is significantly shorter than the only other such reported contact in the Au(III) coordination polymer, [KAuCl$_4$(C$_{10}$H$_8$N$_2$)]$_\infty$ [3.6805 (10) Å].[59] Notably, this interaction between gold and potassium in **9** is also more closely comparable to the corresponding Cu−K distance in **4** [3.0057(4) Å] than the Ag−K bond length of **6** [3.1594(9) Å].

Although compound **9** may be prepared reliably by loss of THF from compound **8**, and compound **9** is converted quantitatively to **8** when redissolved in the ether solvent (Scheme 4), all attempts to elaborate its direct synthesis in a similar manner to compounds **4** and **6** were unsuccessful. Reaction of **1** with K[Au(CN)$_2$] in benzene or a mixture of benzene and THF consistently resulted in the generation of a purple solution, analysis of which by ^{1}H NMR spectroscopy indicated the formation of a complex mix of products, the most predominant of which (59% isolated yield) was the earlier observed potassium dicyanoaluminate (**7**), which was identified by crystallization and a unit cell check.

A notable commonality across all five potassium group 11 bis(alumanyl)metalate structures reported in this study is the consistency of the Al−N bond lengths within the [{SiN^{Dipp}}Al] moieties, which lie across a very narrow range [1.844(3) to 1.876(3) Å], regardless of coinage metal identity. While these values represent a marginal shortening of these bonds in comparison to those of the Al(I) reagent **1** [range 1.887(2) − 1.892(2) Å], they are significantly longer than those observed in [{SiN^{Dipp}}AlI] [1.782(1) and 1.790(1) Å],[39] in which the aluminum center may be unambiguously assigned as in the +3 oxidation state and maintains a 3-coordinate geometry. Such a naive attribution of the +3 oxidation state to aluminum in any of the current metalate species would also necessitate an unreasonable M(3−) assignment to the various group 11 centers. It is notable, however, that the intermediate Al−N bond lengths presented by these species are more closely comparable to those observed in the Al−Al bonded derivative, [{SiN^{Dipp}}Al]$_2$ [1.8426(10) and 1.8458(10) Å].[60] This latter structural observation, thus, argues that these compounds are feasibly better assigned as Al(II) species with significant covalency ascribed to the various group 11-Al interactions. To further address this issue and the broader questions posed at the outset of this work, the coinage metal (CM) species, **2′**, **4**, **5′**, **6**, **8′** and **9** (where **2′**, **5′** and **8′** are the anionic metalate components of compounds **2**, **5** and **8**, respectively) were optimized with density functional theory at the BP86/BS2//

https://doi.org/10.1021/acs.organomet.4c00460
Organometallics XXXX, XXX, XXX−XXX

BP86/BS1 level of theory, and subsequently analyzed with the electronic structure method Atoms in Molecules (AIM) (see Table 2, Figure 6 and the Supporting Information for full

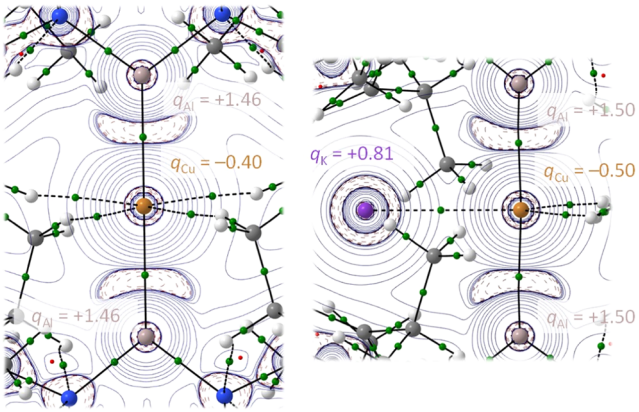

Figure 6. Laplacian plots and selected atomic charges of DFT-optimized **2′** (*left*) and **4** (*right*) structures, computed at the BP86/BS2//BP86/BS1 level of theory.

details). Particular consideration was applied to the most appropriate metal oxidation states that may be ascribed to the CM and Al atoms within the bis(alumanyl)metalate anions and to assess the nature and impact of the K···CM interactions characterized in the contact ion pair structures of **4**, **6** and **9**.

The optimized structures of the potassium bis(alumanyl)-metalates **4**, **6** and **9** were identified to be in reasonable agreement with the crystallographic data where, for instance, only minor elongations of the CM−Al (**4**, 2.0%; **6**, 1.7%; **9**, 2.7%) and CM−K interatomic distances (**4**, 2.6%; **6**, 1.1%; **9**, 2.0%) are observed. Subsequent AIM analysis revealed appreciable CM−Al bond critical points (BCPs) with negative Laplacians, $\nabla^2\rho(r)$ (**4**: $\rho(r)$ = 0.0526, $\nabla^2\rho(r)$ = −0.0400; **6**: $\rho(r)$ = 0.0514, $\nabla^2\rho(r)$ = −0.0334; **9**: $\rho(r)$ = 0.0575, $\nabla^2\rho(r)$ = −0.0226), emblematic of bonds with a large degree of covalent character. Moreover, and consistent with the crystallographic inferences, the calculated atomic charges (**4**: q(Cu) = −0.50, q(Al) = +1.50; **6**: q(Ag) = −0.63, q(Al) = +1.56; **9**: q(Au) = −1.28, q(Al) = +1.87) are indicative of CM(−I) and Al(II) oxidation states in each compound. A series of weaker K−CM BCPs were identified with positive Laplacian values (**4**: $\rho(r)$ = 0.0129, $\nabla^2\rho(r)$ = 0.0366; **6**: $\rho(r)$ = 0.0128, $\nabla^2\rho(r)$ = 0.0389; **9**: $\rho(r)$ = 0.0156, $\nabla^2\rho(r)$ = 0.0525) indicating a more electrostatic nature with predominant charge contraction toward the participating nuclei. Although these electrostatic interactions characterized by AIM are insufficient to designate the K^+ ion as a participating Z-type ligand, it is reasonable to suggest that the constructive $nd_{CM} \rightarrow 4s_K$ donation may serve to further stabilize the unusually charge-dense and otherwise unstable coinage metal centers in this trio of compounds.

The optimized bis(alumanyl)metalate anions, **2′**, **5′**, **8′**, were also identified to be in reasonable agreement with the crystallographic data, albeit with a minor elongation of the Al−CM bonds (**4**$^-$, 3.2%; **6**$^-$, 0.9%). The corresponding CM−Al BCPs, were found to be largely unchanged with respect to their contact ion pair analogues, while the computed atomic charges of the CMs are marginally less negative in **2′**, **5′**, **8′**. (**2′**: q(Cu) = −0.40, q(Al) = +1.46; **5′**: q(Ag) = −0.57, q(Al) = +1.54; **8′**: q(Au) = −1.23, q(Al) = +1.85). Notably, and in all likelihood providing a similar level of stabilization, all six compounds presented a series of BCPs with a similar density threshold between the group 11 centers and methyl groups of the Dipp substituents of the SiN^{Dipp} spectator ligands.

Access to Al(II) Radical Reactivity. As outlined above, the observation of the THF activation product **3** suggests that Al(I) to Al(II) oxidation may be competitive with bis-(alumanyl)metalate formation, either subsequent to or coincident with the KCN metathesis required by either outcome. The theoretical attribution of formal Al(II) character to the aluminum centers of the diamagnetic group 11 compounds, thus, prompted us to consider whether these species could themselves be exploited as governable sources of the [{SiN^{Dipp}}Al$^\bullet$] radical under mild stimulus.

While the spectroscopic observation of fleeting aluminum radicals and under matrix isolation conditions dates from over half a century ago,[61] the "on demand" generation of such species has rarely been achieved. Two recent reports of compounds related to **1**, however, have highlighted the potential of such species to effect unusual reactivity (Scheme 5). Andrada and co-workers have demonstrated that reduction of the diamidoaluminum iodide (**XIII**) with excess KC_8 in benzene does not yield the intended alumanyl product. Rather, these conditions provide for Birch-type reduction of the solvent and the isolation of the cyclohexa-1,4-diene product

Scheme 5. Andrada's Reductive Protocol and Aldridge's Photolytic Method for the Generation of Al(II) Radicals

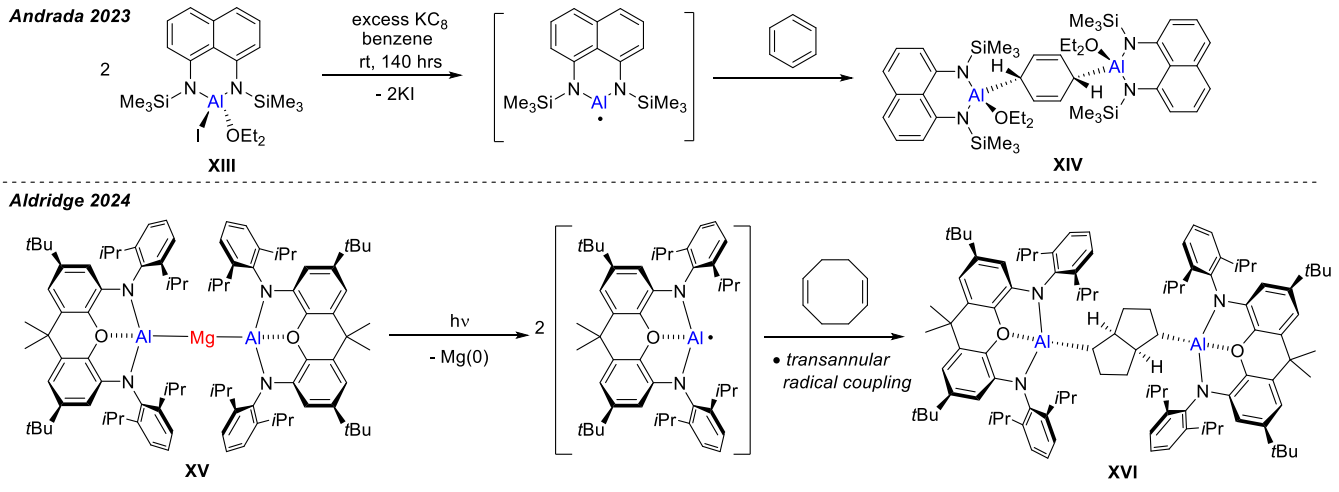

https://doi.org/10.1021/acs.organomet.4c00460
Organometallics XXXX, XXX, XXX−XXX

Scheme 6. Photolysis of 6 Leading to the Unselective Reduction of Benzene and the Stoichiometric Synthesis of Compound 10

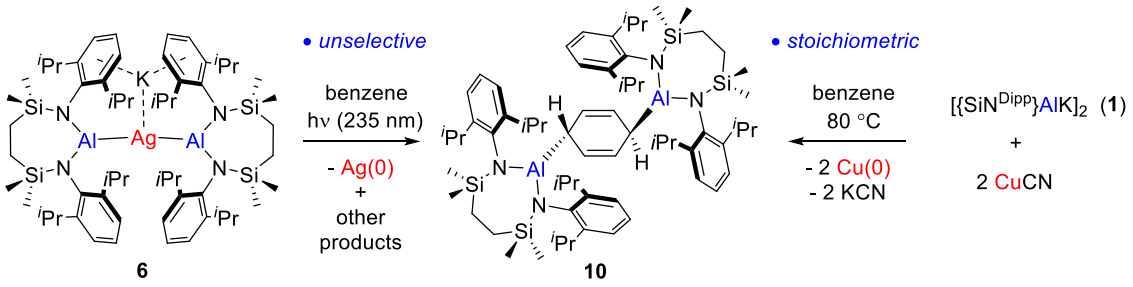

(**XIV**) through reactivity that was deduced to occur through the stepwise addition of the Al(II) radical.[62] Of relevance to the current interpretation of the bonding across the various {Al(II)-M(I)-Al(II)}$^-$ metalate species described above, the group of Aldridge has very recently suggested that the homoleptic magnesium bis(alumanyl), [{($_{xanth}$NON)Al}$_2$Mg] (**XV**, $_{xanth}$NON = [4,5-(NDipp)$_2$-2,7-*t*-Bu$_2$-9,9-Me$_2$-xanthene]$^{2-}$) is best considered as an {Al(II)−Mg(0)−Al(II)} system.[63] Consistent with this viewpoint, photolytic activation of **XV** initiated magnesium metal elimination through the generation of the aluminum radicals. Although unreactive toward benzene, the resultant [($_{xanth}$NON)Al$^•$] radicals induced the transannular coupling of 1,5-cyclooctadiene and the formation of **XVI** in 32% isolated yield (Scheme 5). Although the respective products of these reductive (**XIV**) and photolytic (**XVI**) processes were diamagnetic, both works presented EPR spectroscopic evidence for the intermediacy of the proposed Al-centered radicals.

The electronegative character of the group 11 metals employed in this study prompted us to consider whether bis(alumanyl)metalate photolysis could also provide a selective entry point to Al(II) radical reactivity. The charge-separated species, [({SiN^{Dipp}}Al)$_2$Ag]$^-$[K(THF)$_6$]$^+$ (**5**), was, thus, selected for initial study due to its notable sensitivity to light but relative ease of synthesis. Irradiation of a sample of **5** in d_8-THF with a 235 nm lamp for 30 min induced the formation of a gray precipitate. Analysis of the resultant solution by ^{1}H NMR spectroscopy indicated the formation of a range of soluble products comprising several asymmetric {SiN^{Dipp}} ligand environments. Although potentially indicative of the formation of a KCN-free analogue of the THF ring opened product (**3**), this solution proved intractable toward the identification of any reaction product. Photoactivation of a further solution of the analogous contact ion pair derivative (**6**) in C_6D_6 provided a comparable visual outcome and a similarly complex mixture of products when subsequently assessed by ^{1}H NMR spectroscopy (Scheme 6). Slow evaporation of this benzene solution, however, provided a mixture of crystalline solids, mechanical separation of which yielded several single crystals of compound **10** that were suitable for X-ray diffraction analysis. The results of this analysis, shown in Figure 7 with selected bond length and angle data provided in the figure caption, revealed that **10** is the cyclohexa-1,4-dienyl product resulting from the apparent addition of two [{SiN^{Dipp}}Al] units at the carbocyclic 3- and 6-positions. The structure of compound **10** is, thus, closely comparable to Andrada's recently reported derivative **XIV** and consistent with the proposed photolytic generation of aluminum-centered [SiN^{Dipp}Al$^•$] radicals. This assessment is most clearly borne out by comparison of the C−C bond lengths at the respective 1- and 4-positions of the {C$_6$H$_6$}$^{2-}$

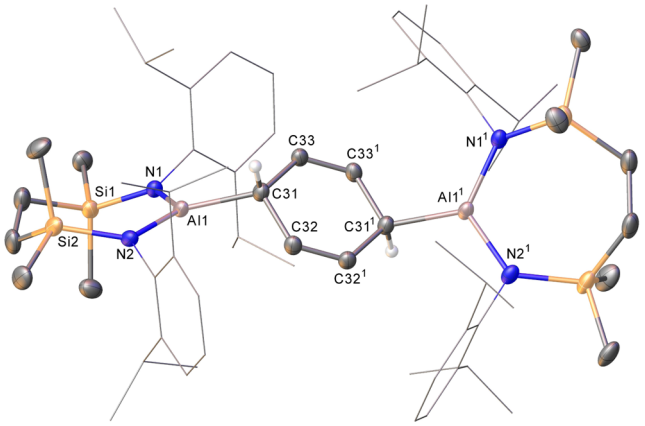

Figure 7. Plot depicting the structure of **10**. Ellipsoids are shown at 30% probability. Solvent and hydrogen atoms (H31 excepted) have been omitted and peripheral substituents are depicted as wireframes, for clarity. Symmetry operations: ^{1} x, $^3/_2 - y$, $^3/_2 - z$. Selected bond lengths (Å) and angles (deg): Al1−N1 1.8019(12), Al1−N2 1.8021(11), Al1−C31 1.9820(15), C31−C32 1.5079(18), C31−C33 1.5028(18), C32−C32^1 1.325(3), C33−C33^1 1.324(3), N1−Al1−N2 118.65(6), N1−Al1−C31 124.37(6), N2−Al1−C31 116.56(6).

moieties in **10** [C32−C32^1 1.325(3), C33−C33^1 1.324(3) Å] and **XIV** [1.333(2) Å], which are unambiguously indicative of localized C═C double bonds in both compounds. Although the Al−C bond of the centrosymmetric structure of **10** [Al1−C31 1.9820(15) Å] is marginally shorter than the analogous metric reported for **XIV** [1.9925(9) Å], this feature may be attributed to the maintenance of a strict 3-coordinate geometry at aluminum, which contrasts with the previously described ether-coordinated structure (Scheme 5).[62]

Although the benzene reduction process to provide **10** is superficially similar to that observed by Andrada and co-workers, it should be emphasized that the synthesis of **XIV** was achieved through an explicit Al(III) to Al(II) reduction, whereas the photolysis of **5** presents greater commonality with Aldridge and co-workers' exploitation of **XV** (Scheme 6). In contrast to the two electrons accounted for by the elimination of magnesium from **XV**, however, the photolytic conversion of compound **5**, or any of the species described herein, to any putative [{SiN^{Dipp}}Al$^•$] radical is necessarily limited to a maximum of 50% due to the anionic bis(alumanyl)metalate formulation and the single electron required to effect the complete elimination of the elemental group 11 metal (Scheme 6).

With this latter consideration in mind, we redirected our attention toward the potential for [{SiN^{Dipp}}Al$^•$] radical generation evident from the isolation of compound **3** in

https://doi.org/10.1021/acs.organomet.4c00460
Organometallics XXXX, XXX, XXX−XXX

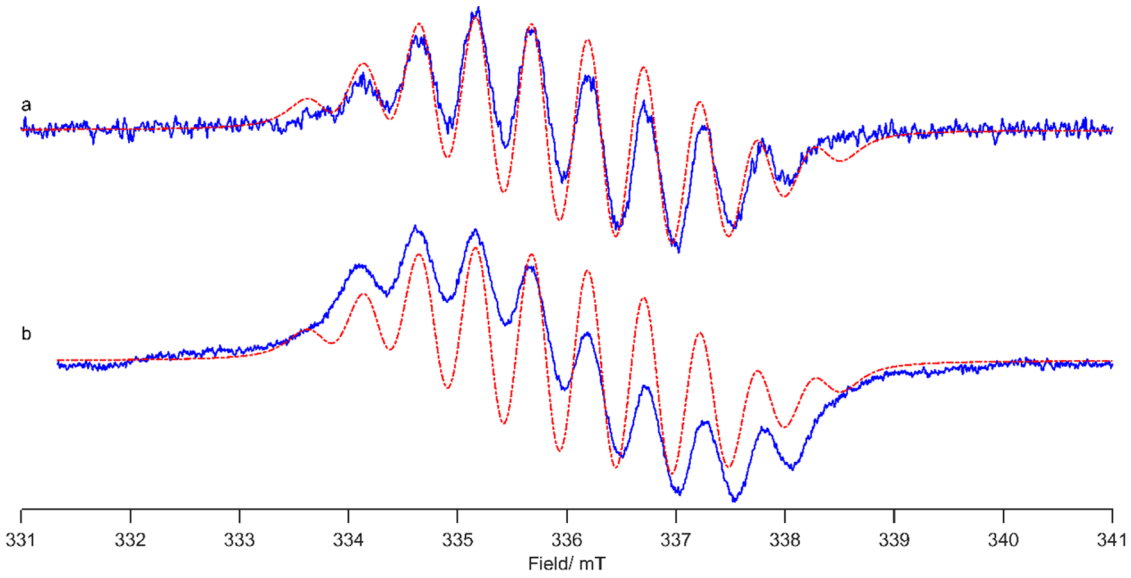

Figure 8. CW X-band EPR spectra (blue) and simulations (red) of a reaction of **1** with CuCN (2 equiv) in mesitylene solvent with added benzene; (a) room temperature reaction, (b) heated to 80 °C for 1 h.

THF (Scheme 1). The development of an appropriate protocol was achieved by iterative variation of the reaction conditions and it was identified that heating of a benzene solution of compound **1** and CuCN at 80 °C provided for the slow, but effectively stoichiometric, generation of compound **10** over the course of 36 h (Scheme 6). Although we have no detailed rationale for this result, it underscores our initial deduction that the observation of either Cu−Al bond formation or Cu(I) reduction arises from competitive processes that may be kinetically discriminated by variation of the reaction conditions.

The resultant isolation of bulk samples of compound **10** also allowed its characterization by NMR spectroscopy. A distinctive and slightly broadened (2H) singlet at δ 2.91 ppm and a multiplet (4H, δ 6.94−6.62 ppm) were, thus, assigned as the respective sp^3 and sp^2 proton environments of the cyclohexadiendiide moiety in the ^{1}H NMR spectrum. These signals, like the corresponding ^{13}C NMR frequencies (δ 32.0 and 121.2 ppm, identified by an HSQC experiment), are closely comparable to the analogous data reported for **XIV** (δ_H 2.37, 5.89; δ_C 29.9, 124.6 ppm) with any minor perturbations again most readily attributed to the lower coordination number of the aluminum center of **10**.

The reactivity of **1** toward CuCN (in mesitylene solvent but in the presence of benzene) was monitored by EPR spectroscopy in an attempt to verify the inferred generation of aluminum radical species. The resultant experimental spectra (Figure 8) were characterized by the spin Hamiltonian parameters g_{iso} = 2.0015, with hyperfine splitting arising from coupling to two equivalent nitrogen nuclei on the {SiN^{Dipp}} ligand backbone with magnitude $a_{iso}(^{14}N)$ = 14.4 MHz (^{14}N, 99.6% abundance, I = 1), and further hyperfine lines arising from coupling to a single aluminum nucleus, a_{iso} (^{27}Al) = 14.4 MHz (^{27}Al, 100% abundance, I = 5/2). Analysis of the hyperfine coupling values permitted determination of the spin density distribution by comparison to the theoretical isotropic hyperfine values for 100% *s*-orbital occupation ($a_0(^{14}N)$ = 1827 MHz, and $a_0(^{27}Al)$ = 3949 MHz), yielding % *s*-orbital densities, ρ_{spin}, of 0.79 (^{14}N) and 0.36 (^{27}Al), respectively. Notably, the magnitude of the ^{27}Al coupling for this radical intermediate is significantly smaller than the radical reported by the Andrada group following reduction of **XIII** with KC_8 ($a_{iso}(^{27}Al)$ = 45.76 MHz; ρ_{spin} = 1.16%),[62] but is comparable to that reported by Aldridge and co-workers,[63] following photoactivation of **XV** ($a_{iso}(^{27}Al)$ = 12 MHz; ρ_{spin} = 0.31%). Interpretation of the aluminum hyperfine coupling suggests more ligand-based spin character,[64] while the low spin density calculated for the nitrogen nuclei indicates that the majority of the electron spin is localized elsewhere on the resulting radical intermediate. Given the notable stability and proven resistance to reduction of the {SiN^{Dipp}} ligand itself, therefore, we suggest that this interpretation is most likely indicative of singly aluminated benzene product, [{SiN^{Dipp}}Al(C_6H_6)$^{\bullet}$]. Although this deduction requires further investigation, in common with the stepwise mechanism calculated by Andrada and co-workers,[62] such a species represents an intermediate en route to compound **10**, which, thus, plausibly results from the addition of two [{SiN^{Dipp}}Al$^{\bullet}$] radicals to the arene solvent.

CONCLUSIONS

In summary, we report that use of coinage metal (CM) cyanide starting materials, either CuCN, AgCN or K[Au(CN)$_2$], in conjunction with the nucleophilic alumanyl derivative, [{SiN^{Dipp}}AlK]$_2$, can provide metathetical access to a series of "alumina-Gilman" reagents [({SiN^{Dipp}}Al)$_2$CM]K. In a majority of cases, the latter species may be isolated in both charge-separated, when crystallized in the presence of THF, or contact ion-paired forms. Although both manifestations are evidently energetically similar, the nature of the CM-to-aluminum interactions is little perturbed, irrespective of the close contact between the K$^+$ center and the electron rich CM metal in the contact paired formulation. This supposition is supported by DFT and QTAIM analysis, which apportion a high degree of covalency to the CM−Al metal bonding and an attribution of an oxidation state to the group 13 center that is best represented as Al(II). This latter inference is supported by both the experimental observation of THF activation, deduced to result from the competitive single electron reduction of the group 11 center during the synthesis of the bis(alumanyl)-metalate products, and the behavior of the photolabile silver

https://doi.org/10.1021/acs.organomet.4c00460
Organometallics XXXX, XXX, XXX−XXX

analog under UV photolysis. Although this latter process proves unselective, a product of 2-fold Al(II) radical addition to benzene has been identified and a more rational, albeit slow, synthesis has been devised through a modification of the reaction that gave rise to the initially identified cuprate metathesis product. The intermediacy of [{SiN^{Dipp}}Al$^{\bullet}$] radicals, which are proposed to add to benzene in a stepwise manner, is supported by the observation of *in situ* recorded EPR spectra, the simulated parameters of which have been assigned to the singly aluminated benzene product, [{SiN^{Dipp}}Al(C_6H_6)$^{\bullet}$]. We are continuing to study the reactivity of these unique metalate derivatives and to investigate the potential of compound **10** to itself function as a rational synthon and a "bottleable" source of the [{SiN^{Dipp}}Al$^{\bullet}$] radical.

■ ASSOCIATED CONTENT

Supporting Information

The Supporting Information is available free of charge at https://pubs.acs.org/doi/10.1021/acs.organomet.4c00460.

Experimental procedures and compound characterization, including NMR spectra, details of the X-ray and computational analyses (PDF)

Coordinates for all computed structures (XYZ)

Accession Codes

Deposition Numbers 2366574−2366581 contain the supplementary crystallographic data for this paper. These data can be obtained free of charge via the joint Cambridge Crystallographic Data Centre (CCDC) and Fachinformationszentrum Karlsruhe Access Structures service.

■ AUTHOR INFORMATION

Corresponding Authors

Michael S. Hill − *Department of Chemistry, University of Bath, Bath BA2 7AY, U.K.*; orcid.org/0000-0001-9784-9649; Email: msh27@bath.ac.uk

Claire L. McMullin − *Department of Chemistry, University of Bath, Bath BA2 7AY, U.K.*; orcid.org/0000-0002-4924-2890; Email: cm2025@bath.ac.uk

Mary F. Mahon − *Department of Chemistry, University of Bath, Bath BA2 7AY, U.K.*; Email: chsmfm@bath.ac.uk

Authors

Han-Ying Liu − *Department of Chemistry, University of Bath, Bath BA2 7AY, U.K.*

Jakub Kenar − *Department of Chemistry, University of Bath, Bath BA2 7AY, U.K.*

Samuel E. Neale − *Department of Chemistry, University of Bath, Bath BA2 7AY, U.K.*

Marta Garofalo − *Department of Chemistry, University of Bath, Bath BA2 7AY, U.K.*

Emma Richards − *School of Chemistry, Cardiff University, Cardiff CF10 3AT, U.K.*; orcid.org/0000-0001-6691-2377

Complete contact information is available at: https://pubs.acs.org/10.1021/acs.organomet.4c00460

Notes

The authors declare no competing financial interest.

■ ACKNOWLEDGMENTS

The authors gratefully acknowledge the Leverhulme Trust Project Award (RPG-2023-104) "Alkaline Element Z-type Ligands for Tunable Base Metal Catalysis" and the University of Bath's Research Computing Group (doi.org/10.15125/b6cd-s854) for their support in this work. This research made use of the Anatra High Throughput Computing (HTC) Cluster at the University of Bath. The authors gratefully acknowledge the University of Bath's Research Computing Group (doi.org/10.15125/b6cd-s854) for their support in this work. We also thank Prof. Ching-Wen Chiu and Yu-Jiang Lin for helpful conversations.

■ REFERENCES

(1) Yoshikai, N.; Nakamura, E. Mechanisms of Nucleophilic Organocopper(I) Reactions. *Chem. Rev.* **2012**, *112* (4), 2339−2372.

(2) Davies, R. P. The structures of lithium and magnesium organocuprates and related species. *Coord. Chem. Rev.* **2011**, *255* (11−12), 1226−1251.

(3) Woodward, S. Decoding the 'black box' reactivity that is organocuprate conjugate addition chemistry. *Chem. Soc. Rev.* **2000**, *29* (6), 393−401.

(4) Kleeberg, C.; Feldmann, E.; Hartmann, E.; Vyas, D. J.; Oestreich, M. Copper-Catalyzed 1,2-Addition of Nucleophilic Silicon to Aldehydes: Mechanistic Insight and Catalytic Systems. *Chem. - Eur. J.* **2011**, *17* (48), 13538−13543.

(5) Delvos, L. B.; Vyas, D. J.; Oestreich, M. Asymmetric Synthesis of -Chiral Allylic Silanes by Enantioconvergent-Selective Copper(I)-Catalyzed Allylic Silylation. *Angew. Chem., Int. Ed.* **2013**, *52* (17), 4650−4653.

(6) Delvos, L. B.; Hensel, A.; Oestreich, M. McQuade's Six-Membered NHC-Copper(I) Complexes for Catalytic Asymmetric Silyl Transfer. *Synthesis* **2014**, *46* (21), 2957−2964.

(7) Lee, K. S.; Hoveyda, A. H. Enantioselective Conjugate Silyl Additions to Cyclic and Acyclic Unsaturated Carbonyls Catalyzed by Cu Complexes of Chiral N-Heterocyclic Carbenes. *J. Am. Chem. Soc.* **2010**, *132* (9), 2898−2899.

(8) Lee, K. S.; Wu, H.; Haeffner, F.; Hoveyda, A. H. NHC-Cu-Catalyzed Silyl Conjugate Additions to Acyclic and Cyclic Dienones and Dienoates. Efficient Site-, Diastereo- and Enantioselective Synthesis of Carbonyl-Containing Allylsilanes. *Organometallics* **2012**, *31* (22), 7823−7826.

(9) Pace, V.; Rae, J. P.; Procter, D. J. Cu(I)-NHC Catalyzed Asymmetric Silyl Transfer to Unsaturated Lactams and Amides. *Org. Lett.* **2014**, *16* (2), 476−479.

(10) Kleeberg, C.; Cheung, M. S.; Lin, Z. Y.; Marder, T. B. Copper-Mediated Reduction of CO_2 with pinB-$SiMe_2$Ph via CO_2 Insertion into a Copper-Silicon Bond. *J. Am. Chem. Soc.* **2011**, *133* (47), 19060−19063.

(11) Sgro, M. J.; Piers, W. E.; Romero, P. E. Synthesis, structural characterization and thermal properties of copper and silver silyl complexes. *Dalton Trans.* **2015**, *44* (8), 3817−3828.

(12) McCarty, B. J.; Thomas, B. M.; Zeller, M.; Van Hoveln, R. Synthesis of a Copper Silyl Complex by Disilane Activation. *Organometallics* **2018**, *37* (18), 2937−2940.

(13) Hensel, A.; Nagura, K.; Delvos, L. B.; Oestreich, M. Enantioselective Addition of Silicon Nucleophiles to Aldimines Using a Preformed NHC- Copper(I) Complex as the Catalyst. *Angew. Chem., Int. Ed.* **2014**, *53* (19), 4964−4967.

(14) Li, Z. H.; Zhang, L.; Nishiura, M.; Hou, Z. M. Copper-Catalyzed Umpolung of Imines through Carbon-to-Nitrogen Boryl Migration. *ACS Catal.* **2019**, *9* (5), 4388−4393.

(15) Glockling, F.; Hooton, K. A. Triphenylgermyl complexes of copper, silver and gold. *J. Chem. Soc.* **1962**, 2658−2661.

(16) Orlov, N. A.; Bochkarev, L. N.; Nikitinsky, A. V.; Kropotova, V. Y.; Zakharov, L. N.; Fukin, G. K.; Khorshev, S. Y. Synthesis of germylcopper compounds by hydride method.: Crystal structure of $(C_6F_5)_3GeCu(PPh_3)_2$. *J. Organomet. Chem.* **1998**, *560* (1−2), 21−25.

(17) Piers, E.; Lemieux, R. Reaction of (trimethylgermyl)copper(I)-dimethylsulfide with acyl chlorides. Efficient syntheses of function-

alized acyltrimethylgermanes. *Organometallics* **1995**, *14* (11), 5011−5012.
(18) Piers, E.; Lemieux, R. M. Novel (trimethylgermyl)copper(I) reagents: Preparation and addition to α,β-unsaturated ketones and α,β-alkynic esters. *Organometallics* **1998**, *17* (19), 4213−4217.
(19) Lin, W. D.; You, L. J.; Yuan, W.; He, C. Cu-Catalyzed Enantioselective Hydrogermylation: Asymmetric Synthesis of Unnatural β-Germyl α-Amino Acids. *ACS Catal.* **2022**, *12* (23), 14592−14600.
(20) Charman, R. S. C.; Evans, N. J.; English, L. E.; Neale, S. E.; Vasko, P.; Mahon, M. F.; Liptrot, D. J. The structures and reactivity of NHC-supported copper(I) triphenylgermyls. *Chem. Sci.* **2024**, *15* (2), 584−593.
(21) Bhattacharyya, K. X.; Akana, J. A.; Laitar, D. S.; Berlin, J. M.; Sadighi, J. P. Carbon-carbon bond formation on reaction of a copper(I) stannyl complex with carbon dioxide. *Organometallics* **2008**, *27* (12), 2682−2684.
(22) Charman, R. S. C.; Mahon, M. F.; Lowe, J. P.; Liptrot, D. J. The structures of ring-expanded NHC supported copper(I) triphenylstannyls and their phenyl transfer reactivity towards heterocumulenes. *Dalton Trans.* **2022**, *51* (3), 831−835.
(23) Oestreich, M.; Hartmann, E.; Mewald, M. Activation of the Si-B Interelement Bond: Mechanism, Catalysis, and Synthesis. *Chem. Rev.* **2013**, *113* (1), 402−441.
(24) Heine, A.; Herbstirmer, R.; Stalke, D. $CU_2R_2BRLi(THF)_3$, R = $Si(SiMe_3)_3$: A complex containing 5-coordinate silicon in a 3-center 2-electron bond (THF = tetrahydrofuran). *J. Chem. Soc. Chem. Commun.* **1993**, No. 23, 1729−1731.
(25) Heine, A.; Stalke, D. Preparation and structure of 2 highly reactive intermediates: $Li(THF)_4$ $Cu_5Cl_4R_2$ and $Li(THF)_4AlCl_3R$, R = $Si(SiMe_3)_3$. *Angew. Chem., Int. Ed.* **1993**, *32* (1), 121−122.
(26) Klinkhammer, K. W. Synthesis and crystal structure of the two lithium hypersilylcuprates $LiCu_2[Si(SiMe_3)_3]_3$ and $[Li_7(Ot\text{-}Bu)_6][Cu_2\{Si(SiMe_3)_3\}_3$. *Z. Anorg. Allg. Chem.* **2000**, *626* (5), 1217−1223.
(27) Lerner, H. W.; Scholz, S.; Bolte, M. The sodium cuprate $(t\text{-}Bu_3Si)_2CuNa$: Formation and X-ray crystal structure analysis. *Organometallics* **2001**, *20* (3), 575−577.
(28) Klinkhammer, K. W.; Klett, J.; Xiong, Y.; Yao, S. L. Homo- and heteroleptic hypersilylcuprates - Valuable reagents for the synthesis of molecular compounds with a Cu-Si bond. *Eur. J. Inorg. Chem.* **2003**, *2003* (18), 3417−3424.
(29) Plotzitzka, J.; Kleeberg, C. (18-C-6)K(NC)Cu(I)$SiMe_2Ph$, a Potassium Silylcyanocuprate as a Catalyst Model for Silylation Reactions with Silylboranes: Syntheses, Structures, and Catalytic Properties. *Inorg. Chem.* **2017**, *56* (11), 6671−6680.
(30) Orlov, N. A.; Bochkarev, L. N.; Nikitinsky, A. V.; Zhiltsov, S. F.; Zakharov, L. N.; Fukin, G. K.; Khorshev, S. Y. Synthesis and crystal structure of cationic complex of ytterbium with organogermanium cuprate anions $\{Yb(THF)_6\}^{2+}(Ph_3Ge)_2Cu_2^-\}\cdot 2THF$. *J. Organomet. Chem.* **1997**, *547* (1), 65−69.
(31) Oda, H.; Morizawa, Y.; Oshima, K.; Nozaki, H. Regioselctive germylcupration of acetylenes. *Tetrahedron Lett.* **1984**, *25* (30), 3217−3220.
(32) Segawa, Y.; Yamashita, M.; Nozaki, K. Boryllithium: Isolation, characterization, and reactivity as a boryl anion. *Science* **2006**, *314* (5796), 113−115.
(33) Yamashita, M.; Suzuki, Y.; Segawa, Y.; Nozaki, K. Synthesis, structure of borylmagnesium, and its reaction with benzaldehyde to form benzoylborane. *J. Am. Chem. Soc.* **2007**, *129* (31), 9570−9751.
(34) Segawa, Y.; Yamashita, M.; Nozaki, K. Boryl anion attacks transition-metal chlorides to form boryl complexes: Syntheses, spectroscopic, and structural studies on group 11 borylmetal complexes. *Angew. Chem., Int. Ed.* **2007**, *46* (35), 6710−6713.
(35) Hicks, J.; Vasko, P.; Goicoechea, J. M.; Aldridge, S. Synthesis, structure and reaction chemistry of a nucleophilic aluminyl anion. *Nature* **2018**, *557* (7703), 92−95.
(36) Schwamm, R. J.; Anker, M. D.; Lein, M.; Coles, M. P. Reduction vs. Addition: The Reaction of an Aluminyl Anion with 1,3,5,7-Cyclooctatetraene. *Angew. Chem., Int. Ed.* **2019**, *58* (5), 1489−1493.
(37) Koshino, K.; Kinjo, R. Construction of sigma-Aromatic AlB2 Ring via Borane Coupling with a Dicoordinate Cyclic (Alkyl)-(Amino)Aluminyl Anion. *J. Am. Chem. Soc.* **2020**, *142* (19), 9057−9062.
(38) Kurumada, S.; Takamori, S.; Yamashita, M. An alkyl-substituted aluminium anion with strong basicity and nucleophilicity. *Nat. Chem.* **2020**, *12* (1), 36−39.
(39) Schwamm, R. J.; Coles, M. P.; Hill, M. S.; Mahon, M. F.; McMullin, C. L.; Rajabi, N. A.; Wilson, A. S. S. A Stable Calcium Alumanyl. *Angew. Chem., Int. Ed.* **2020**, *59* (10), 3928−3932.
(40) Jackson, R. A.; Matthews, A. J. R.; Vasko, P.; Mahon, M. F.; Hicks, J.; Liptrot, D. J. An acyclic aluminyl anion. *Chem. Commun.* **2023**, *59* (35), 5277−5280.
(41) Hicks, J.; Vasko, P.; Goicoechea, J. M.; Aldridge, S. The Aluminyl Anion: A New Generation of Aluminium Nucleophile. *Angew. Chem., Int. Ed.* **2021**, *60* (4), 1702−1713.
(42) Coles, M. P. Aluminyl Anions. *Encycl. Inorg. Bioinorg. Chem.* **2011**, 1−23.
(43) Schmidt, E. S.; Jockisch, A.; Schmidbaur, H. A carbene analogue with low-valent gallium as a heteroatom in a quasi-aromatic imidazolate anion. *J. Am. Chem. Soc.* **1999**, *121* (41), 9758−9759.
(44) Baker, R. J.; Jones, C.; Kloth, M.; Platts, J. A. Oxidative coupling of an anionic gallium(I) carbene analogue: Synthesis and structural characterization of an unprecedented pi-cyclopentadienyl-bridged digallane complex. *Organometallics* **2004**, *23* (21), 4811−4813.
(45) Coles, M. P.; Evans, M. J. The emerging chemistry of the aluminyl anion. *Chem. Commun.* **2023**, *59* (5), 503−519.
(46) Schwamm, R. J.; Anker, M. D.; Lein, M.; Coles, M. P.; Fitchett, C. M. Indyllithium and the Indyl Anion InL^-: Heavy Analogues of N-Heterocyclic Carbenes. *Angew. Chem., Int. Ed.* **2018**, *57* (20), 5885−5887.
(47) Griffin, L. P.; Ellwanger, M. A.; Crumpton, A. E.; Roy, M. M. D.; Heilmann, A.; Aldridge, S. Mercury-Group 13 Metal Covalent Bonds: A Systematic Comparison of Aluminyl, Gallyl and Indyl Metallo-ligands. *Angew. Chem., Int. Ed.* **2024**, *63* (23), No. e202404527.
(48) Okuno, Y.; Yamashita, M.; Nozaki, K. Borylcyanocuprate in a One-Pot Carboboration by a Sequential Reaction with an Electron-Deficient Alkyne and an Organic Carbon Electropile. *Angew. Chem., Int. Ed.* **2011**, *50* (4), 920−923.
(49) Okuno, Y.; Yamashita, M.; Nozaki, K. One-Pot Carboboration of Alkynes Using Lithium Borylcyanocuprate and the Subsequent Suzuki-Miyaura Cross-Coupling of the Resulting Tetrasubstituted Alkenylborane. *Eur. J. Org. Chem.* **2011**, *2011* (20−21), 3951−3958.
(50) Kajiwara, T.; Terabayashi, T.; Yamashita, M.; Nozaki, K. Syntheses, structures, and reactivities of borylcopper and -zinc compounds: 1,4-silaboration of an alpha,beta-unsaturated ketone to form a gamma-siloxyallylborane. *Angew. Chem., Int. Ed.* **2008**, *47* (35), 6606−6610.
(51) Liu, H. Y.; Schwamm, R. J.; Hill, M. S.; Mahon, M. F.; McMullin, C. L.; Rajabi, N. A. Ambiphilic Al-Cu Bonding. *Angew. Chem., Int. Ed.* **2021**, *60* (26), 14390−14393.
(52) Jones, C.; Mills, D. P.; Rose, R. P.; Stasch, A.; Woodul, W. D. Synthesis and further reactivity studies of some transition metal gallyl complexes. *J. Organomet. Chem.* **2010**, *695* (22), 2410−2417.
(53) Green, S. P.; Jones, C.; Mills, D. P.; Stasch, A. Group 9 and 11 metal(I) gallyl complexes stabilized by N-heterocyclic carbene coordination: First structural characterization of Ga-M (M = Cu or Ag) bonds. *Organometallics* **2007**, *26* (14), 3424−3430.
(54) McManus, C.; Crumpton, A. E.; Aldridge, S. Alkyne insertion into Cu-Al bonds and selective functionalization to form copper acyl compounds. *Chem. Commun.* **2022**, *58* (59), 8274−8277.
(55) Liu, H. Y.; Neale, S. E.; Hill, M. S.; Mahon, M. F.; McMullin, C. L. On the reactivity of Al-group 11 (Cu, Ag, Au) bonds. *Dalton Trans.* **2022**, *51* (10), 3913−3924.

https://doi.org/10.1021/acs.organomet.4c00460
Organometallics XXXX, XXX, XXX−XXX

(56) McManus, C.; Hicks, J.; Cui, X. L.; Zhao, L. L.; Frenking, G.; Goicoechea, J. M.; Aldridge, S. Coinage metal aluminyl complexes: probing regiochemistry and mechanism in the insertion and reduction of carbon dioxide. *Chem. Sci.* **2021**, *12* (40), 13458−13468.
(57) Hicks, J.; Mansikkamaki, A.; Vasko, P.; Goicoechea, J. M.; Aldridge, S. A nucleophilic gold complex. *Nat. Chem.* **2019**, *11* (3), 237−241.
(58) Jansen, M. The chemistry of gold as an anion. *Chem. Soc. Rev.* **2008**, *37* (9), 1826−1835.
(59) Song, C.; Li, Y.-Z.; Chen, Y.-Q.; Xiao, S.-J.; You, X.-Z. Poly[[terachlorogold(III)potassium(I)(Au-K)]-[μ]-4,4′-bipyridine]. *Acta Cryst. E* **2004**, *E60* (12), m1741−m1743.
(60) Schwamm, R. J.; Hill, M. S.; Liu, H. Y.; Mahon, M. F.; McMullin, C. L.; Rajabi, N. A. Seven-Membered Cyclic Potassium Diamidoalumanyls. *Chem. - Eur. J.* **2021**, *27* (60), 14971−14980.
(61) Uhl, W.; Layh, M. Formal Oxidation State + 2: Metal−Metal Bonded Versus Mononuclear Derivatives. *Group 13 Met. Alum., Gallium, Indium Thallium* **2011**, 246−284.
(62) Mandal, D.; Demirer, T. I.; Sergeieva, T.; Morgenstern, B.; Wiedemann, H. T. A.; Kay, C. W. M.; Andrada, D. M. Evidence of AlII Radical Addition to Benzene. *Angew. Chem., Int. Ed.* **2023**, *62* (13), No. e202217184.
(63) Griffin, L. P.; Ellwanger, M. A.; Clark, J.; Myers, W. K.; Roper, A. F.; Heilmann, A.; Aldridge, S. Bis(Aluminyl)Magnesium: a Source of Nucleophilic or Radical Aluminium-Centred Reactivity. *Angew. Chem., Int. Ed.* **2024**, *63* (22), No. e202405053.
(64) Kaim, W. Single electron transfer reaction of aluminum hydride with nitrogen-containing heterocycles. ESR characterization of the radical products. *J. Am. Chem. Soc.* **1984**, *106* (6), 1712−1716.

https://doi.org/10.1021/acs.organomet.4c00460
Organometallics XXXX, XXX, XXX−XXX